

Supporting Information

Mouysset *et al.* 10.1073/pnas.0805944105

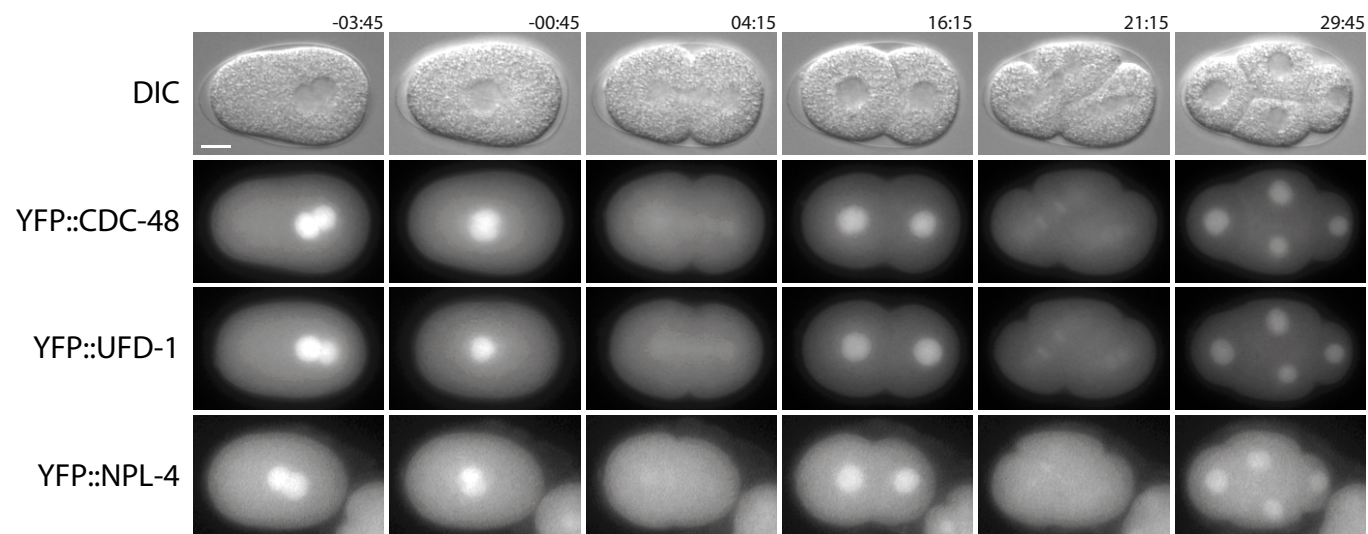


Fig. S1. CDC-48, UFD-1, and NPL-4 form a complex localized in the nucleus of early embryos. DIC and fluorescent images of transgenic wild-type embryos expressing YFP::CDC-48, YFP::UFD-1, and YFP::NPL-4. Representative DIC images correspond to YFP::CDC-48. (Scale bar, 10 μ m).

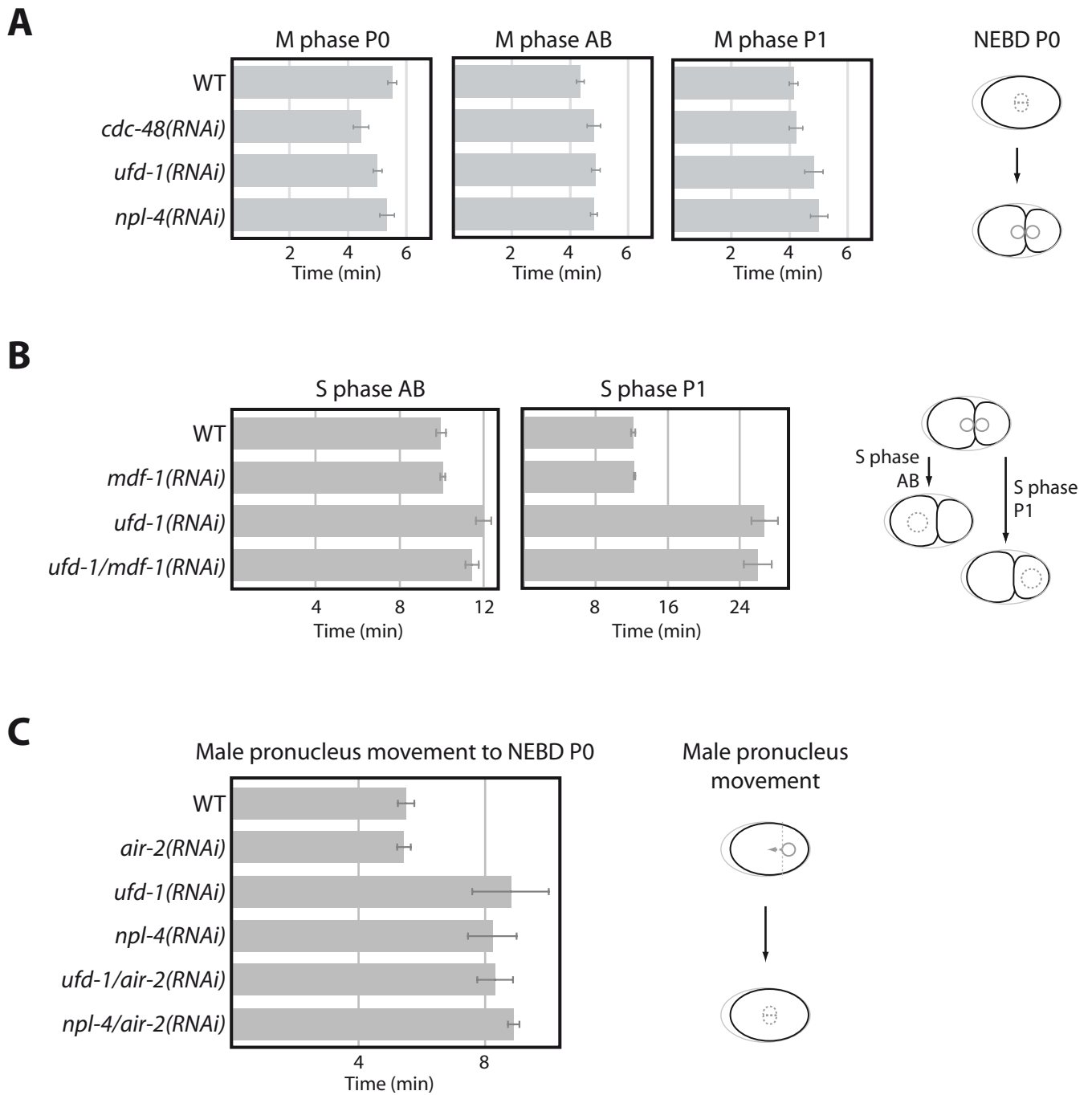


Fig. S2. Downregulation of $CDC-48^{UFD-1/NPL-4}$ does not influence mitosis progression. (A) Quantification of mitosis time of P0, AB, and P1 cells in wild-type (WT) or the indicated RNAi embryos. Mitosis corresponds to the time between onset of NEBD and the end of cytokinesis (see cartoon at right). (B) Quantification of S phase duration in AB and P1 cells after downregulation of *mdf-1* and/or *ufd-1*. (C). Quantification of the time separating initiation of male pronucleus movement from the end of cytokinesis (see cartoon at right) for epistatic analysis of *air-2(RNAi)* with *ufd-1(RNAi)* or *npl-4(RNAi)*.

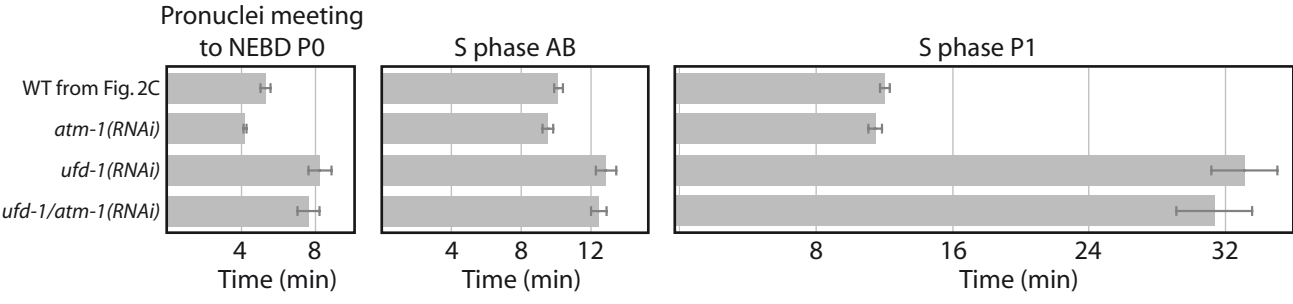


Fig. S3. Downregulation of ATM-1 does not suppress the S phase delay caused by UFD-1 depletion. Quantification of S phase duration in P0, AB, and P1 cells after downregulation of *atm-1* and/or *ufd-1*.

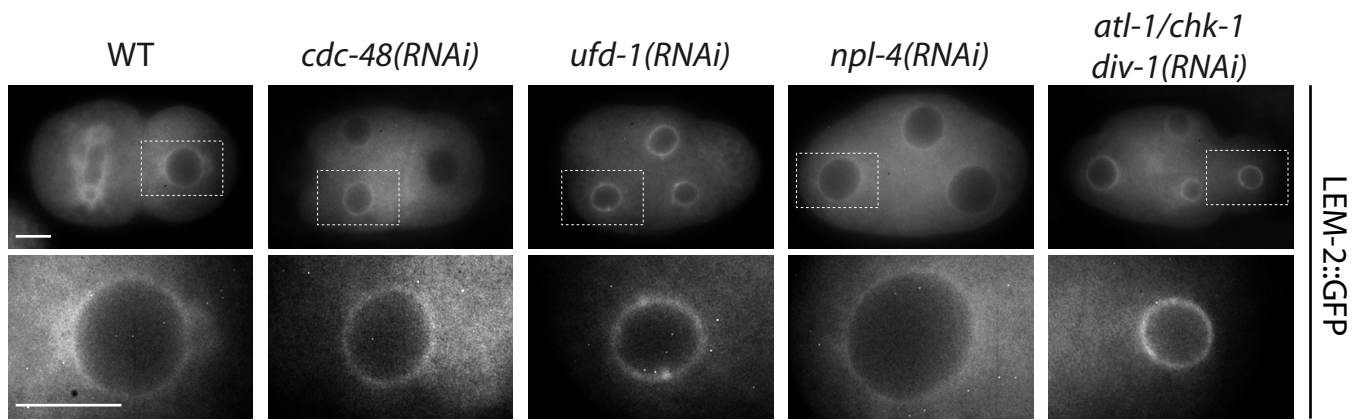


Fig. S4. Depletion of CDC-48^{UFD-1/NPL-4} does not influence the nuclear envelope integrity. Fluorescent images of transgenic embryos expressing LEM-2::GFP in wild-type (WT) or the indicated RNAi embryos. (Scale bar, 10 μ m).

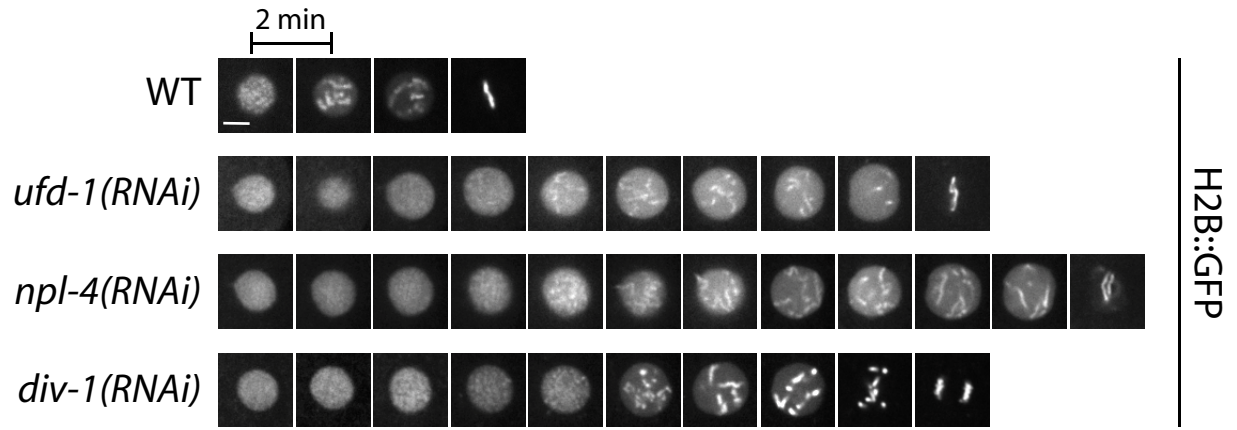
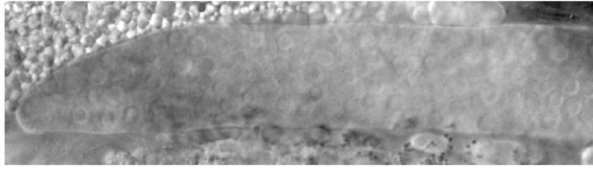


Fig. S5. Delayed chromatin condensation in embryos depleted for UFD-1, NPL-4, and DIV-1. Images of P1 cell nuclei of wild-type (WT), *ufd-1(RNAi)*, *npl-4(RNAi)*, and *div-1(RNAi)* embryos expressing H2B::GFP. Images were taken at two-minute intervals. The first image is taken 10 min after anaphase onset in P0 cells. (Scale bar, 5 μm).

Control

DIC



npl-4(RNAi)



DAPI (blue)
 α RAD-51 (red)

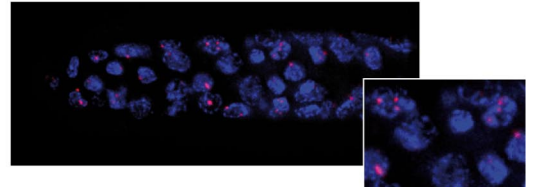
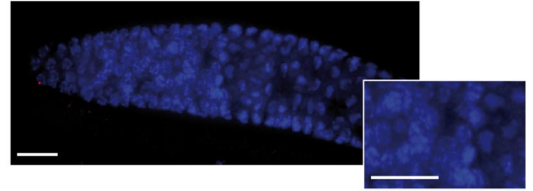


Fig. S6. Formation of RAD-51 foci in the germline of *npl-4(RNAi)* hermaphrodite worms. DIC and fluorescence images of gonads of *npl-4(RNAi)* worms. (Scale bar, 10 μ m).

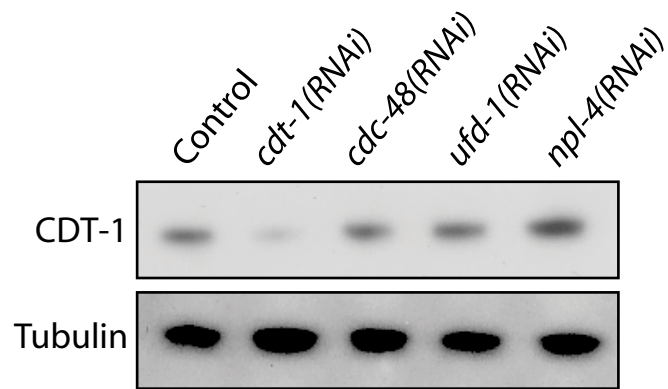


Fig. S7. Levels of CDT-1 are not regulated by the CDC-48^{UFD-1/NPL-4} complex. Protein extracts of the indicated strains were analyzed by immunoblotting with CDT-1-specific antibodies. Tubulin was used as loading control.

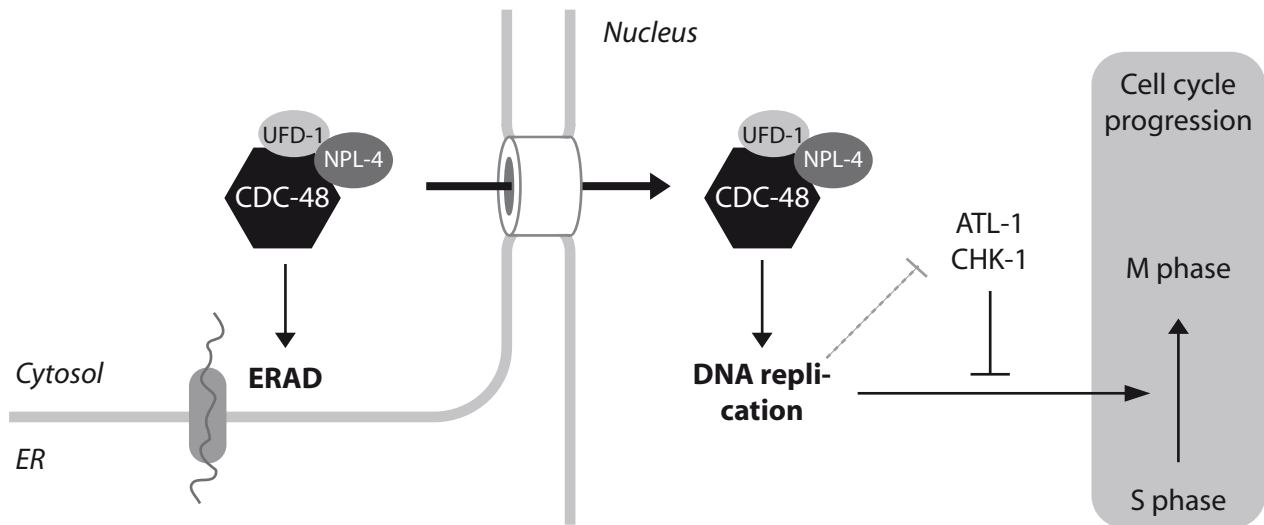
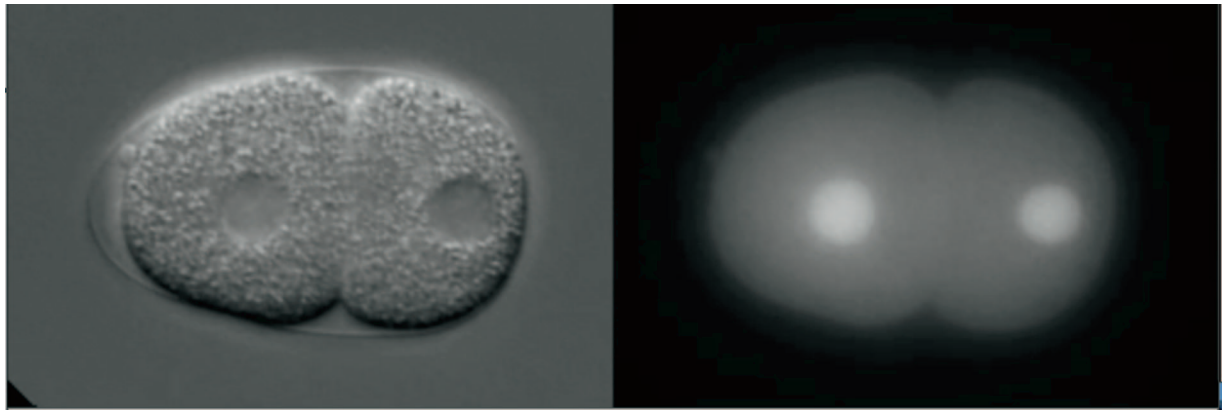
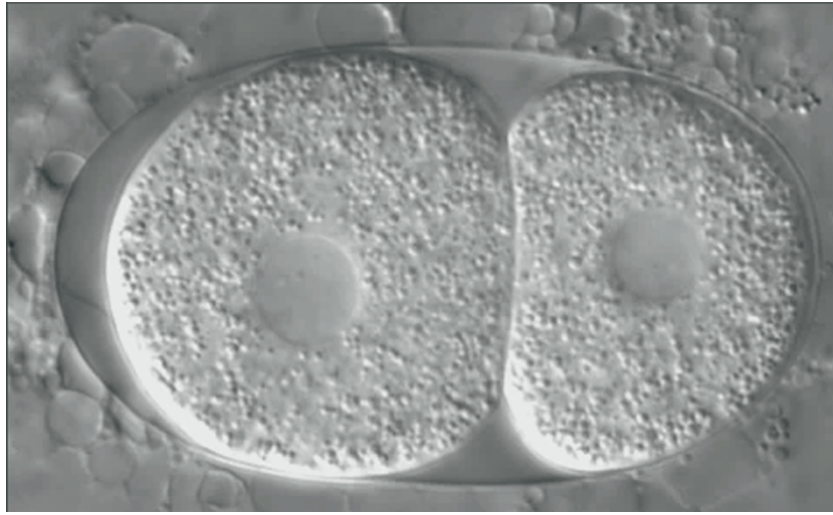


Fig. S8. Model for a role of CDC-48^{UFD-1/NPL-4} in DNA replication. Independent of its well characterized function in ERAD, the CDC-48^{UFD-1/NPL-4} complex shuttles into the nucleus at the end of M phase to regulate DNA replication. Consequently, replication defects in S phase caused by depletion of CDC-48^{UFD-1/NPL-4} activate the checkpoint kinases ATL-1 and CHK-1 to arrest the cell cycle.



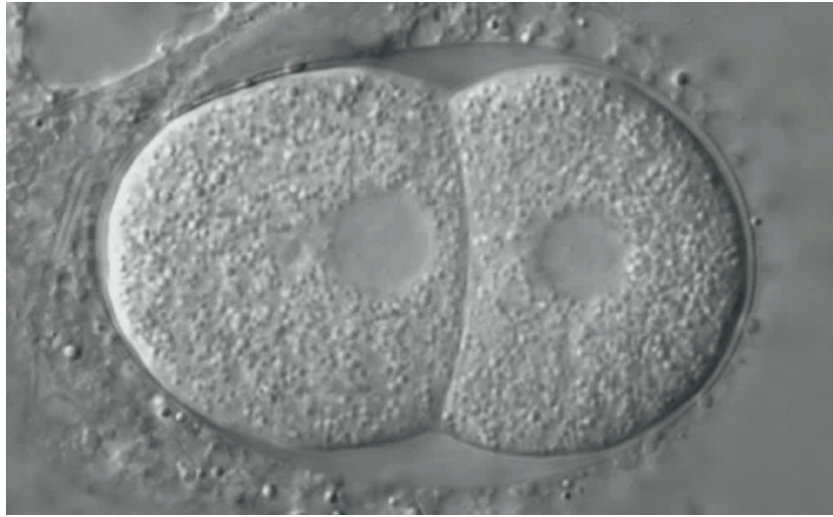
Movie S1. This movie corresponds to experiments shown in Fig. 1 A and Fig. S1 and illustrates the early division up to the four-cell stage of a *C. elegans* embryo expressing YFP::CDC-48 by DIC and fluorescence microscopy. The localization patterns of YFP::UFD-1 and YFP::NPL-4 are similar to YFP::CDC-48 (QuickTime, 2.4 MB).

[Movie S1 \(MOV\)](#)



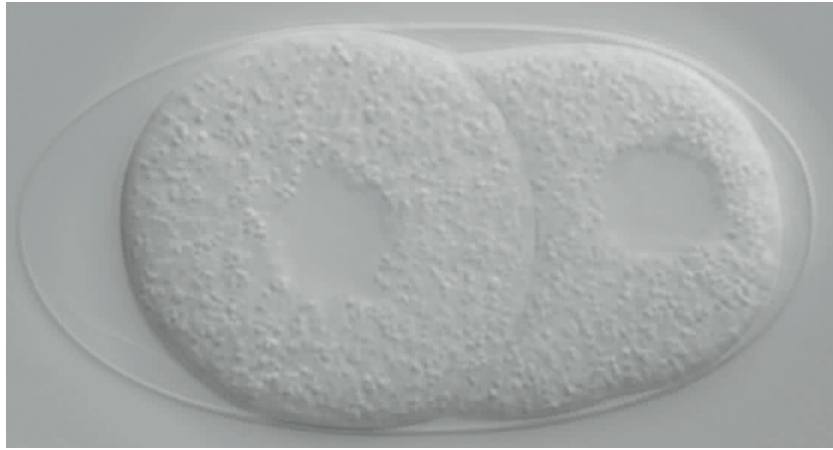
Movie S2. This movie corresponds to the experiment shown in Fig. 1B and illustrates the early division up to the four-cell stage of a wild-type *C. elegans* embryo by DIC microscopy (QuickTime, 5.0 MB).

[Movie S2 \(MOV\)](#)



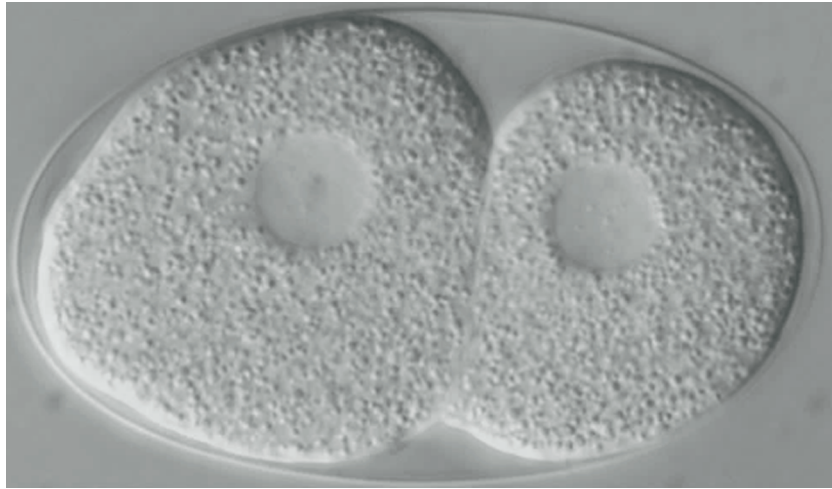
Movie S3. This movie corresponds to the experiment shown in Fig. 1B and illustrates by the early division up to the four-cell stage of a *cdc-48(RNAi)* *C. elegans* embryo DIC microscopy. It clearly reveals an abnormal persistent three-cell stage (QuickTime, 6.8 MB).

[Movie S3 \(MOV\)](#)



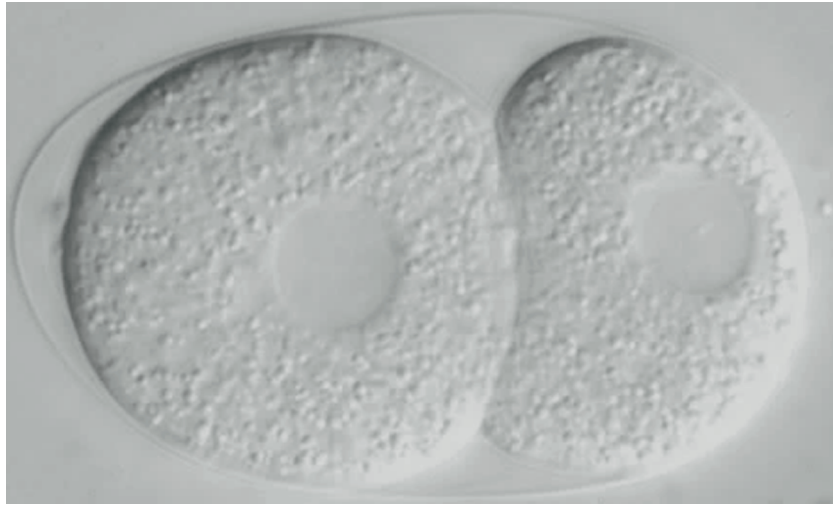
Movie S4. This movie corresponds to the experiment shown in Fig. 1B and illustrates the early division up to the four-cell stage of a *ufd-1(RNAi)* *C. elegans* embryo by DIC microscopy. It clearly reveals an abnormal persistent three-cell stage (QuickTime, 3.8 MB).

[Movie S4 \(MOV\)](#)



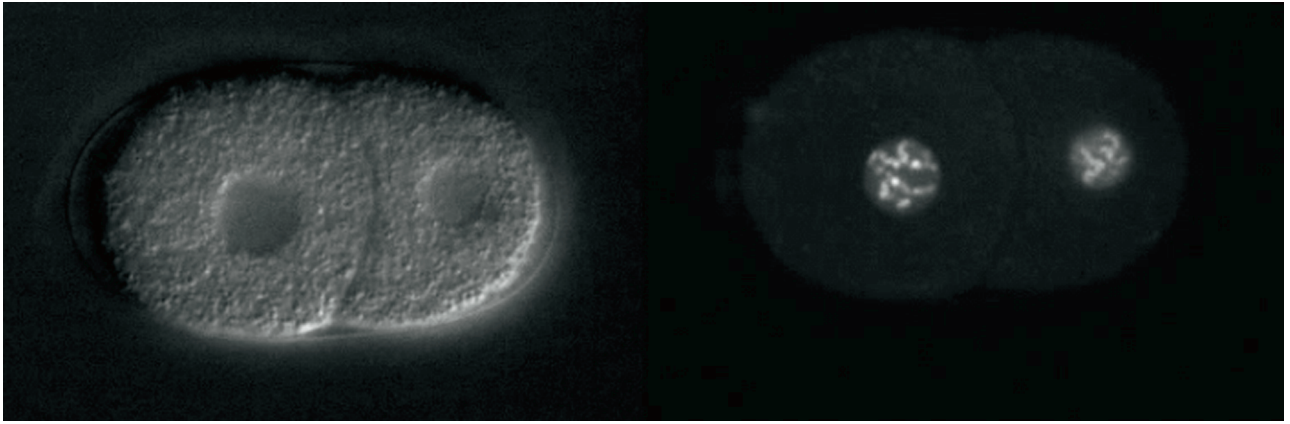
Movie 55. This movie corresponds to the experiment shown in Fig. 1B and illustrates the early division up to the four-cell stage of an *npl-4(RNAi)* *C. elegans* embryo by DIC microscopy. It clearly reveals an abnormal persistent three-cell stage (QuickTime, 5.3 MB).

[Movie 55 \(MOV\)](#)



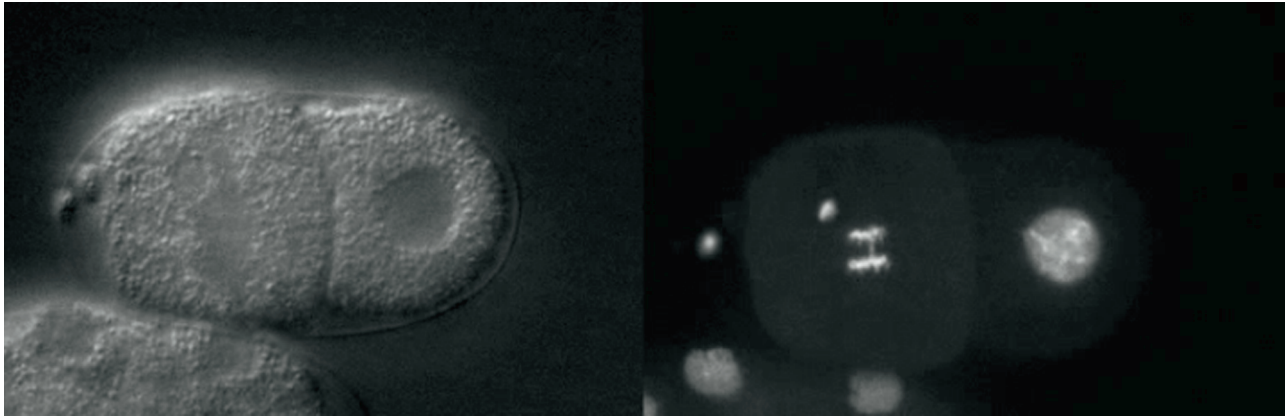
Movie S6. This movie corresponds to the experiment shown in Fig. 2A and illustrates the early division up to the four-cell stage of a *cdc-48/atl-1(RNAi)* *C. elegans* embryo by DIC microscopy. It displays that the abnormal persistent P1 cell division delay of *cdc-48(RNAi)* embryos is significantly suppressed (QuickTime, 2.5 MB).

[Movie S6 \(MOV\)](#)



Movie S7. This movie corresponds to experiments shown in Fig. 3A and Fig. S5 and illustrates the early division up to the four-cell stage of a wild-type *C. elegans* embryo expressing H2B::GFP by DIC and fluorescence microscopy (QuickTime, 4.1 MB).

[Movie S7 \(MOV\)](#)



Movie S8. This movie corresponds to the experiment shown in Fig. 3A and Fig. S5 and illustrates the early division up to the four-cell stage of a *npl-4(RNAi)* *C. elegans* embryo expressing H2B::GFP by DIC and fluorescence microscopy. It displays chromosome bridges during mitosis as well as a delay in chromatin condensation, especially in the P1 cell (QuickTime, 4.9 MB).

[Movie S8 \(MOV\)](#)

Table S1. Statistical data and analysis

Fig.	Genotype	n	Time duration, min:s	SEM, min:s	t test (P value)		
					WT	<i>ufd-1(RNAi)</i>	<i>npl-4(RNAi)</i>
Duration of the cell division delay between AB and P1 cells							
1C	WT	21	02:02	0:06	—	1×10^{-16}	6×10^{-11}
	<i>ubxn-1(RNAi)</i>	8	01:56	0:10	7×10^{-01}	2×10^{-07}	n.d.
	<i>cdc-48(RNAi)</i>	13	14:32	1:08	8×10^{-06}	2×10^{-01}	2×10^{-02}
	<i>ufd-1(RNAi)</i>	35	21:27	1:14	1×10^{-16}	—	9×10^{-01}
	<i>npl-4(RNAi)</i>	19	21:52	2:17	6×10^{-11}	9×10^{-01}	—
	<i>ufd-1/npl-4(RNAi)</i>	13	22:50	1:06	2×10^{-21}	5×10^{-01}	7×10^{-01}
1D	<i>sel-1(RNAi)</i>	11	02:12	0:07	3×10^{-01}	3×10^{-08}	n.d.
	<i>ufd-1(RNAi)</i>	8	21:53	2:16	1×10^{-14}	—	n.d.
	<i>ire-1(RNAi)</i>	10	02:08	0:04	4×10^{-01}	9×10^{-08}	n.d.
	<i>ufd-1/ire-1(RNAi)</i>	11	22:46	1:25	8×10^{-20}	7×10^{-01}	n.d.
4E	WT	7	01:52	0:06	—	3×10^{-09}	n.d.
	<i>ufd-1(RNAi)</i>	7	16:41	0:53	3×10^{-09}	—	n.d.
	<i>cdt-1(RNAi)</i>	12	03:00	0:11	4×10^{-04}	2×10^{-12}	n.d.
	<i>cdc-6(RNAi)</i>	16	06:04	0:15	5×10^{-10}	2×10^{-12}	n.d.
Duration from pronuclei meeting to NEBD in P0 cell							
2C	WT	9	05:18	0:15	—	4×10^{-01}	3×10^{-04}
	<i>cdc-48(RNAi)</i>	6	05:53	0:54	5×10^{-01}	6×10^{-14}	6×10^{-02}
	<i>ufd-1(RNAi)</i>	6	08:25	0:38	4×10^{-04}	—	1×10^{-00}
	<i>npl-4(RNAi)</i>	6	08:22	0:36	3×10^{-04}	1×10^{-20}	—
	<i>cdc-48/atl-1(RNAi)</i>	2	03:49	0:18	4×10^{-02}	1×10^{-01}	9×10^{-03}
	<i>ufd-1/atl-1(RNAi)</i>	10	03:43	0:07	3×10^{-05}	6×10^{-14}	n.d.
	<i>npl-4/atl-1(RNAi)</i>	5	03:43	0:18	2×10^{-03}	n.d.	7×10^{-05}
	<i>ufd-1/chk-1(RNAi)</i>	6	04:27	0:10	3×10^{-02}	1×10^{-01}	n.d.
	<i>npl-4/chk-1(RNAi)</i>	8	05:15	0:23	9×10^{-01}	n.d.	1×10^{-03}
	<i>ufd-1/atl-1/chk-1(RNAi)</i>	2	04:26	0:05	2×10^{-01}	2×10^{-01}	n.d.
	<i>npl-4/atl-1/chk-1(RNAi)</i>	5	04:37	0:38	3×10^{-01}	n.d.	4×10^{-03}
S3	WT (as in Fig. 2C)	—	—	—	n.d.	n.d.	n.d.
	<i>atm-1(RNAi)</i>	11	04:10	0:05	4×10^{-04}	4×10^{-06}	n.d.
	<i>ufd-1(RNAi)</i>	10	08:14	0:37	1×10^{-03}	—	n.d.
	<i>ufd-1/atm-1(RNAi)</i>	9	07:37	0:36	4×10^{-03}	5×10^{-01}	n.d.
Duration of the interphase in AB cell							
2C	WT	23	10:08	0:15	—	7×10^{-06}	5×10^{-09}
	<i>cdc-48(RNAi)</i>	9	11:49	0:33	4×10^{-03}	4×10^{-01}	1×10^{-02}
	<i>ufd-1(RNAi)</i>	22	12:26	0:22	7×10^{-06}	—	1×10^{-02}
	<i>npl-4(RNAi)</i>	17	14:05	0:29	5×10^{-09}	1×10^{-02}	—
	<i>cdc-48/atl-1(RNAi)</i>	3	09:43	0:23	6×10^{-01}	2×10^{-02}	2×10^{-03}
	<i>ufd-1/atl-1(RNAi)</i>	13	11:09	0:33	7×10^{-02}	6×10^{-02}	n.d.
	<i>npl-4/atl-1(RNAi)</i>	9	11:51	0:22	1×10^{-03}	n.d.	6×10^{-03}
	<i>ufd-1/chk-1(RNAi)</i>	12	11:23	0:10	3×10^{-03}	5×10^{-02}	n.d.
	<i>npl-4/chk-1(RNAi)</i>	9	11:13	0:22	3×10^{-02}	n.d.	8×10^{-04}
	<i>ufd-1/atl-1/chk-1(RNAi)</i>	10	11:20	0:10	7×10^{-02}	6×10^{-02}	n.d.
<i>npl-4/atl-1/chk-1(RNAi)</i>	8	12:16	0:21	2×10^{-04}	n.d.	3×10^{-02}	
S2B	WT	29	09:59	0:19	—	1×10^{-02}	n.d.
	<i>mdf-1(RNAi)</i>	3	10:04	0:22	9×10^{-01}	1×10^{-04}	n.d.
	<i>ufd-1(RNAi)</i>	3	12:01	0:07	1×10^{-02}	—	n.d.
	<i>ufd-1/mdf-1(RNAi)</i>	11	11:27	0:14	2×10^{-03}	6×10^{-01}	n.d.
S3	WT (as in Fig. 2C)	—	—	—	n.d.	n.d.	n.d.
	<i>atm-1(RNAi)</i>	11	09:32	0:18	2×10^{-01}	2×10^{-02}	n.d.
	<i>ufd-1(RNAi)</i>	10	12:51	0:35	3×10^{-05}	—	n.d.
	<i>ufd-1/atm-1(RNAi)</i>	13	12:26	0:26	4×10^{-05}	5×10^{-02}	n.d.

Fig.	Genotype	n	Time duration, min:s	SEM, min:s	t test (P value)		
					WT	<i>ufd-1(RNAi)</i>	<i>npl-4(RNAi)</i>
Duration of the interphase in P1 cell							
2C	WT	23	12:15	0:17	—	8×10^{-18}	3×10^{-12}
	<i>cdc-48(RNAi)</i>	9	26:56	1:54	3×10^{-12}	4×10^{-01}	5×10^{-03}
	<i>ufd-1(RNAi)</i>	22	28:52	1:08	8×10^{-18}	—	6×10^{-03}
	<i>npl-4(RNAi)</i>	17	34:01	1:14	3×10^{-12}	6×10^{-03}	—
	<i>cdc-48/atl-1(RNAi)</i>	3	13:13	1:10	3×10^{-01}	7×10^{-05}	5×10^{-06}
	<i>ufd-1/atl-1(RNAi)</i>	13	18:04	0:54	2×10^{-08}	3×10^{-07}	n.d.
	<i>npl-4/atl-1(RNAi)</i>	9	19:15	0:49	6×10^{-11}	n.d.	6×10^{-08}
	<i>ufd-1/chk-1(RNAi)</i>	12	17:41	0:12	4×10^{-14}	6×10^{-08}	n.d.
	<i>npl-4/chk-1(RNAi)</i>	9	18:22	0:34	3×10^{-11}	n.d.	1×10^{-08}
	<i>ufd-1/atl-1/chk-1(RNAi)</i>	10	15:51	0:28	2×10^{-07}	3×10^{-08}	n.d.
<i>npl-4/atl-1/chk-1(RNAi)</i>	8	19:08	0:35	5×10^{-12}	n.d.	1×10^{-07}	
3D	WT	29	12:09	0:15	—	2×10^{-08}	8×10^{-21}
	<i>div-1(RNAi)</i>	14	17:11	0:09	4×10^{-16}	2×10^{-13}	5×10^{-10}
	<i>ufd-1(RNAi)</i>	39	30:48	0:48	2×10^{-28}	—	1×10^{-00}
	<i>npl-4(RNAi)</i>	12	30:52	1:25	8×10^{-21}	1×10^{-00}	—
	<i>ufd-1/div-1(RNAi)</i>	13	32:45	1:11	2×10^{-24}	2×10^{-01}	n.d.
	<i>npl-4/div-1(RNAi)</i>	12	35:53	1:07	6×10^{-27}	n.d.	2×10^{-02}
S2B	WT (as in Fig. 3D)	—	—	—	n.d.	n.d.	n.d.
	<i>mdf-1(RNAi)</i>	3	12:20	0:05	8×10^{-01}	2×10^{-03}	n.d.
	<i>ufd-1(RNAi)</i>	3	26:45	1:28	3×10^{-15}	—	n.d.
	<i>ufd-1/mdf-1(RNAi)</i>	11	26:01	1:32	1×10^{-15}	8×10^{-01}	n.d.
S3	WT (as in Fig. 2C)	—	—	—	n.d.	n.d.	n.d.
	<i>atm-1(RNAi)</i>	11	11:41	0:24	3×10^{-01}	1×10^{-09}	n.d.
	<i>ufd-1(RNAi)</i>	10	33:07	1:55	7×10^{-16}	—	n.d.
	<i>ufd-1/atm-1(RNAi)</i>	13	31:22	2:11	9×10^{-13}	6×10^{-01}	n.d.
Duration of the mitosis in P0 cell							
S2A	WT	22	05:31	0:09	—	3×10^{-02}	2×10^{-01}
	<i>cdc-48(RNAi)</i>	9	04:17	0:16	9×10^{-04}	7×10^{-02}	8×10^{-02}
	<i>ufd-1(RNAi)</i>	20	05:01	0:09	3×10^{-02}	—	6×10^{-01}
	<i>npl-4(RNAi)</i>	14	05:10	0:07	2×10^{-01}	6×10^{-01}	—
Duration of the mitosis in AB cell							
S2A	WT	23	04:21	0:08	—	2×10^{-02}	1×10^{-02}
	<i>cdc-48(RNAi)</i>	13	04:49	0:14	8×10^{-02}	8×10^{-01}	1×10^{-00}
	<i>ufd-1(RNAi)</i>	28	04:53	0:09	2×10^{-02}	—	7×10^{-01}
	<i>npl-4(RNAi)</i>	23	04:46	0:07	1×10^{-02}	7×10^{-01}	—
Duration of the mitosis in P1 cell							
S2A	WT	23	04:08	0:09	—	7×10^{-02}	9×10^{-03}
	<i>cdc-48(RNAi)</i>	13	04:13	0:14	8×10^{-01}	2×10^{-01}	7×10^{-02}
	<i>ufd-1(RNAi)</i>	27	04:50	0:09	7×10^{-02}	—	7×10^{-01}
	<i>npl-4(RNAi)</i>	24	05:01	0:07	9×10^{-03}	7×10^{-01}	—
Duration from the male pronucleus movement to NEBD in P0 cell							
S2C	WT	7	05:30	0:15	—	1×10^{-02}	6×10^{-03}
	<i>air-2(RNAi)</i>	10	05:26	0:13	9×10^{-01}	3×10^{-03}	1×10^{-03}
	<i>ufd-1(RNAi)</i>	4	08:48	1:12	1×10^{-02}	—	7×10^{-01}
	<i>npl-4(RNAi)</i>	5	08:14	0:46	6×10^{-03}	7×10^{-01}	—
	<i>ufd-1/air-2(RNAi)</i>	11	08:19	0:34	3×10^{-03}	7×10^{-01}	n.d.
	<i>npl-4/air-2(RNAi)</i>	10	08:54	0:11	5×10^{-04}	n.d.	5×10^{-01}

Two-tailed Student's *t* test was used to generate p-values compared to wild-type (WT), *ufd-1(RNAi)*, and *npl-4(RNAi)*. Non determined values are indicated by n.d. *n* represents the number of scored embryos, time durations and SEM are expressed in min:s.

Table S2. Knockdown of *atl-1* and *chk-1* does not suppress chromosome bridges caused by *ufd-1(RNAi)*

Genotype	<i>n</i>	Percentage values
Proportion of two-, three-, and four-cell stage embryos with chromosome bridges		
WT	15	0
<i>ufd-1(RNAi)</i>	37	43
<i>npl-4(RNAi)</i>	50	68
Proportion of nuclei with chromosome bridges in early embryos		
WT	97	0
<i>ufd-1(RNAi)</i>	98	12
<i>ufd-1/atl-1/chk-1(RNAi)</i>	98	19

Shown is quantification of DAPI stained nuclei with chromosome bridges by confocal microscopy.

Table S3. Values and statistical analysis of replication assay shown in Fig. 4B

Nuclei per one-celled embryo	Control	<i>cdc-48</i> (RNAi)	<i>ufd-1</i> (RNAi)	<i>npl-4</i> (RNAi)	+ HU 20 mM	<i>mus-101</i> (RNAi)	<i>atl-1/chk-1</i> (RNAi)
3	0.19	0.50	0.46	0.42	0.40	0.46	0.51
4	0.16	0.34	0.18	0.35	0.27	0.18	0.31
5	0.09	0.10	0.16	0.13	0.12	0.16	0.11
6	0.10	0.06	0.16	0.03	0.09	0.16	0.04
7	0.15	—	0.04	0.03	0.03	0.04	0.02
8	0.10	—	—	—	0.08	—	—
9	0.06	—	—	—	—	—	—
10	0.03	—	—	0.03	0.01	—	—
12	0.03	—	—	—	—	—	—
13	0.01	—	—	—	—	—	—
14	0.03	—	—	—	—	—	—
15	0.01	—	—	—	—	—	—
16	0.01	—	—	—	—	—	—
17	—	—	—	—	—	—	—
18	0.02	—	—	—	—	—	—
21	0.01	—	—	—	—	—	—
Mean	6.67	3.72	4.13	4.06	4.39	4.30	3.76
SD	3.67	0.88	1.27	1.48	1.67	1.51	0.98
SEM	0.36	0.12	0.17	0.27	0.19	0.28	0.15
<i>n</i>	106	50	56	31	75	30	45
99% CI	5.73 to 7.61	3.39 to 4.05	3.67 to 4.58	3.33 to 4.80	3.88 to 4.90	3.54 to 5.06	3.36 to 4.15
Min.	3	3	3	3	3	3	3
Median	6	3.5	4	4	4	4	3
Max.	21	6	7	10	10	8	7

Shown is the distribution of embryos determined from the number of nuclei per one-celled embryo after cytochalasin B treatment. Mean, standard deviation (SD), standard error of the mean (SEM), number of embryos (*n*), confidence interval (CI) at 99%, minimal value (Min.), median value, and maximal value (Max.) as indicated.